

Article

Negativity of the Casimir self-entropy in spherical geometries

Yang Li ^{1,†}, Kimball A. Milton ^{2,†,*}, Prachi Parashar ^{3,†}, and Lujun Hong ⁴

¹ Department of Physics, Nanchang University, Nanchang 330031, China; leon@ncu.edu.cn

² Homer L. Dodge Department of Physics and Astronomy, University of Oklahoma, Norman, OK 73019 USA; kmilton@ou.edu

³ John A. Logan College, Carterville, IL 62918 USA; Prachi.Parashar@jalc.edu

⁴ Institute of Space Science and Technology, Nanchang University, Nanchang, 330031, China

* Correspondence: kmilton@ou.edu

† These authors contributed equally to this work.

Abstract: It has been recognized for some time that even for perfect conductors, the interaction Casimir entropy, due to quantum/thermal fluctuations, can be negative. This result was not considered problematic because it was thought that the self-entropies of the bodies would cancel this negative interaction entropy, yielding a total entropy that was positive. In fact, this cancellation seems not to occur. The positive self-entropy of a perfectly conducting sphere does indeed just cancel the negative interaction entropy of a system consisting of a perfectly conducting sphere and plate, but a model with weaker coupling in general possesses a regime where negative self-entropy appears. The physical meaning of this surprising result remains obscure. In this paper we re-examine these issues, using improved physical and mathematical techniques, partly based on the Abel-Plana formula, and present numerical results for arbitrary temperatures and couplings, which exhibit the same remarkable features.

Keywords: Casimir free energy; entropy; Abel-Plana formula

1. Introduction

It is ordinarily expected that entropies of closed systems should be positive. This follows from the Boltzmann definition in terms of the number of microstates Ω , so the entropy is given as $S = k_B \ln \Omega$ (k_B is the Boltzmann constant). Quantum-mechanically, in terms of the density operator ρ , the entropy is $S = -k_B \text{Tr } \rho \ln \rho$. But there are intriguing possibilities of negative entropy [1–3].

Here we are considering quantum-fluctuational or Casimir free energies and entropies. For two parallel conducting plates possessing nonzero resistivity, the entropy corresponding to the interaction free energy vanishes at zero temperature, as required by the Nernst heat theorem (third law of thermodynamics). However, for sufficiently low temperatures, compared to the inverse of the plate separation, a region of negative interaction entropy emerges [4]. But the expectation at that time was that the total entropy must be positive. Negative Casimir interaction entropies also occurred without dissipation between a sphere and a plane [5–8], both perfectly conducting, or between two perfectly conducting spheres [9,10]. This was systematically explored in the dipole regime [11,12].

But, indeed, it turned out that the sphere-plane problem was resolved by considering the self-entropy of the plate and the sphere separately. The former vanishes in the perfectly conducting limit, but the latter is just such as to cancel the most negative contribution of the interaction entropy [13,14]. The sphere-sphere entropy is then seen to be clearly positive as well.

However, going beyond the case of a perfectly conducting sphere has proved to be more subtle. We carried out a systematic treatment for an imperfectly conducting sphere, modeled by a δ -function sphere, or a “plasma-sphere,” described by the potential $\mathbf{V} = \epsilon - \mathbf{1} = \lambda(\mathbf{1} - \hat{\mathbf{r}}\hat{\mathbf{r}})$, (in terms of polar coordinates based on the center of the sphere), where the transversality condition is required by Maxwell’s equations. We take the coupling λ to be frequency dependent, according to the plasma model, $\lambda = \lambda_0/(\zeta^2 a)$, where $\zeta = -i\omega$ is the Euclidean frequency, and a is the radius of the sphere. The dimensionless coupling constant λ_0 is necessarily positive. In the limit of $\lambda \rightarrow \infty$ we recover the entropy for a perfectly conducting sphere first obtained by Balian and Duplantier [15]. But for sufficiently weak coupling, even at high temperatures, we found that the entropy could turn negative [16,17]. (The results found there largely agreed with those found subsequently by Bordag and Kirsten [18,19].)

Since the transverse electric contribution to the entropy is always negative, and presents no difficulties in its evaluation, in this paper we concentrate on the transverse magnetic free energy, F_H . One feature of the analysis here is that we always subtract an infrared sensitive, but unphysical term, which we only subtracted in a *ad hoc* manner in Ref. [16]. The most salient element of our new treatment, however, is the emphasis on the Abel-Plana formula, and the numerical computations based upon that formulation. In the next section we give the general formulas for this model, and recast the result in Abel-Plana form, which expresses the finite temperature-dependent part of free energy in terms of a mode sum over the phase of a quantity involving spherical Bessel functions. Then in Sec. 3 we specialize to weak coupling, where the mode sum can be carried out explicitly for the lowest-order term. The result agrees with that found in Ref. [16]. The low-temperature limit is considered in Sec. 4; we extract coincident free energies using both the Euclidean and the (real-frequency) Abel-Plana formulations. We briefly review the previous result for high temperatures in Sec. 5. Finally, we present general numerical results in Sec. 6, which, for coupling and temperature of order unity (in units of $1/a$) turn out to be remarkably similar to those found for low temperature. Further numerical explorations have shown how the analytic asymptotic behaviors are realized. Concluding remarks round out the paper.

In this paper we adopt natural units, with $\hbar = c = k_B = 1$.

2. Transverse magnetic free energy of plasma-shell sphere

We concentrate on the transverse-magnetic (TM) contribution to the free energy of a δ -sphere, since the transverse electric (TE) part seems unambiguous, and always yields a negative contribution to the entropy. As derived in Ref. [16] the TM free energy is given by

$$F_H = \frac{T}{2} \sum_{n=-\infty}^{\infty} e^{in\alpha\tilde{\tau}} \sum_{l=1}^{\infty} (2l+1) P_l(\cos \delta) \ln \left[1 - \lambda_0 \frac{\alpha|n| e'_l(\alpha|n|) s'_l(\alpha|n|)}{\alpha^2 n^2 + \tilde{\mu}^2} \right], \quad (1)$$

where $\tilde{\tau} = \tau/a \rightarrow 0$ is the dimensionless time-splitting regulator, $\delta \rightarrow 0$ is the angular point-splitting regulator, and $\alpha = 2\pi a T$, so that $n\alpha = a\zeta_n$, where ζ_n is the Matsubara frequency. Further we have inserted an infrared regulator $\tilde{\mu} = \mu a$, modeled as a photon mass. Here the modified Riccati-Bessel functions are

$$s_l(x) = \sqrt{\frac{\pi x}{2}} I_{l+1/2}(x), \quad e_l(x) = \sqrt{\frac{2x}{\pi}} K_{l+1/2}(x). \quad (2)$$

We might hope to eliminate the $\tilde{\mu}$ regulator dependence, formally, by subtraction of an unphysical coupling-independent term:

$$F_H = \frac{\alpha}{2\pi a} \sum_{n=0}^{\infty} ' \cos(n\alpha\tilde{\tau}) \sum_{l=1}^{\infty} (2l+1) P_l(\cos \delta) \left(\ln \left[(n\alpha)^2 + \tilde{\mu}^2 - \lambda_0 f_H(l, n\alpha) \right] - \ln \left[(n\alpha)^2 + \tilde{\mu}^2 \right] \right), \quad (3)$$

where the prime on the summation sign means that the $n = 0$ term is to be counted with half weight, and we have abbreviated $f_H(l, x) = xe'_l(x)s'_l(x)$. The subtracted term was evaluated in Ref. [16], because $\sum_{l=1}^{\infty} (2l+1)P_l(\cos \delta) = -1$:

$$F_H^{\text{sub}} = \frac{T}{2} \sum_{n=-\infty}^{\infty} e^{in\alpha\tilde{\tau}} \ln \left[n^2\alpha^2 + \tilde{\mu}^2 \right] = -\frac{1}{2\tilde{\tau}} + T \ln \frac{\mu}{T}. \quad (4)$$

We discarded this term as unphysical (it makes no reference to the properties of the sphere) frequently throughout Ref. [16], although it was not done systematically. Now we propose doing so. Then we can recast the remainder of F_H using the Abel-Plana formula, which reads

$$\sum_{n=0}^{\infty} 'g(n) = \int_0^{\infty} dt g(t) + i \int_0^{\infty} dt \frac{g(it) - g(-it)}{e^{2\pi t} - 1}. \quad (5)$$

Applied to Eq. (3) after the omission of the subtracted term (4), we see that the first integral gives a contribution independent of T , which is the (divergent) zero-temperature TM energy of the sphere [20]. We are here only concerned with the temperature-dependent part, which we can rewrite as

$$\Delta F_H = -\frac{1}{\pi\alpha} \int_0^{\infty} \frac{dx}{e^{2\pi x/\alpha} - 1} \sum_{l=1}^{\infty} (2l+1) \arg[-x^2 - \lambda_0 f_H(l, ix)]. \quad (6)$$

Here, we have dropped the regulators because this expression is finite.

The definition of the argument function is somewhat subtle. We choose it to be defined by the usual arctangent,

$$\arg(z) = \arctan \left(\frac{\Im z}{\Re z} \right), \quad -\frac{\pi}{2} < \arctan y \leq \frac{\pi}{2}, \quad (7)$$

which is discontinuous when $\Re z$ passes through zero. This choice is necessary in order to have a well-defined limit at zero temperature. (See Section 4.2.) It also guarantees that the free energy vanishes for zero coupling, which would seem an obvious physical requirement. Therefore, the argument appearing in Eq. (6) is

$$\arg[-x^2 - \lambda_0 f_H(l, ix)] = \arctan \left(\frac{\lambda_0 \frac{\pi}{2} \mathcal{J}_\nu^2(x)}{-x^2 + \lambda_0 \frac{\pi}{2} \mathcal{J}_\nu(x) \mathcal{Y}_\nu(x)} \right), \quad \nu = l + \frac{1}{2}. \quad (8)$$

The functions appearing here are, in terms of ordinary Bessel functions J_ν and Y_ν ,

$$\mathcal{J}_\nu(x) = -\sqrt{\frac{2x}{\pi}} [xj_l(x)]' = (\nu - 1/2)J_\nu(x) - xJ_{\nu-1}(x), \quad (9a)$$

$$\mathcal{Y}_\nu(x) = -\sqrt{\frac{2x}{\pi}} [xy_l(x)]' = (\nu - 1/2)Y_\nu(x) - xY_{\nu-1}(x), \quad (9b)$$

j_l, y_l being the corresponding spherical Bessel functions.

The ultraviolet convergence of ΔF_H in Eq. (6) in x is assured by the exponential factor, but the convergence in l requires further investigation. It is easily checked that

$$f_H(l, ix) \sim -\frac{\nu}{2} \quad \text{as} \quad l \rightarrow \infty, \quad (10)$$

so

$$\arg[-x^2 - \lambda_0 f_H(l, ix)] \rightarrow 0, \quad \text{as} \quad l \rightarrow \infty. \quad (11)$$

3. Weak coupling

With the above definition of the argument function, we can readily work out the weak coupling expansion of the free energy. The leading term in λ_0 is obtained from the first term in the expansion of the arctangent, so

$$\Delta F_H^{(1)} = \frac{\lambda_0}{\pi a} \int_0^\infty \frac{dx}{x} \frac{1}{e^{2\pi x/\alpha} - 1} \sum_{l=1}^{\infty} (2l+1) ([xj_l(x)]')^2. \quad (12)$$

The sum on l can be carried out using the addition theorem for spherical Bessel functions

$$\sum_{l=0}^{\infty} (2l+1) j_l(x) j_l(y) = \frac{\sin(x-y)}{x-y}. \quad (13)$$

Then, the l sum in Eq. (12) is

$$\lim_{y \rightarrow x} \frac{\partial}{\partial x} \frac{\partial}{\partial y} xy \left[\frac{\sin(x-y)}{x-y} - j_0(x) j_0(y) \right] = 1 + \frac{x^2}{3} - \cos^2 x, \quad (14)$$

since $j_0(x) = \frac{\sin x}{x}$. This yields the same result found in Ref. [16], Eq. (5.34),

$$\Delta F_H^{(1)} = \frac{\lambda_0}{\pi a} \int_0^\infty \frac{dx}{x} \frac{1}{e^{2\pi x/\alpha} - 1} \left(\sin^2 x + \frac{x^2}{3} \right) = \frac{\lambda_0}{4\pi a} \left[\ln \left(\frac{\sinh \alpha}{\alpha} \right) + \frac{\alpha^2}{18} \right], \quad (15)$$

found there both using the Abel-Plana (real frequency) and the Euclidean frequency formulations.

4. Low temperature

4.1. Euclidean frequency argument

Let us first write the subtracted free energy in the original point-splitting form:

$$\Delta F_H = \frac{T}{2} \sum_{n=-\infty}^{\infty} e^{inx} \sum_{l=1}^{\infty} (2l+1) P_l(\cos \delta) \ln[x^2 - \lambda_0 f_H(l, x)], \quad (16)$$

Here $x = 2\pi n a T = n\alpha$. So the low temperature limit corresponds to small x . Using the small-argument expansion for the Bessel functions,

$$f_H(l, x) \sim -\frac{l(l+1)}{2l+1} - \frac{3+2l(l+1)}{(4l^2-1)(2l+3)} x^2 + O(x^4) - x^{2l+1} \left[(-1)^l 2^{-2(l+1)} \frac{(l+1)^2 \pi}{\Gamma(l+3/2)^2} + O(x^2) \right], \quad x \ll 1, \quad (17)$$

so it is seen that the leading odd term in x arises only from the $l = 1$ term, where

$$f_H(1, x) \sim -\frac{2}{3} - \frac{7}{15} x^2 + \frac{4}{9} x^3 + O(x^4), \quad x \ll 1, \quad (18)$$

so the logarithm in the free energy is

$$\ln[x^2 - \lambda_0 f_H(1, x)] \sim \ln \frac{2\lambda_0}{3} + \left(\frac{3}{2\lambda_0} + \frac{7}{10} \right) x^2 - \frac{2}{3} x^3 + O(x^4), \quad x \ll 1. \quad (19)$$

This is the same as Eq. (6.12) of Ref. [16], except the x^2 in the logarithm there has been removed by the subtraction.

The above analysis is relevant to the low temperature behavior because that may be extracted by using the Euler-Maclaurin formula,

$$F_H = T \sum_{n=0}^{\infty} 'g(n) \sim T \int_0^{\infty} dn g(n) - T \sum_{k=1}^{\infty} \frac{B_{2k}}{(2k)!} g^{(2k-1)}(0). \quad (20)$$

Because of the subtraction, the expansion can be carried out around $n = 0$, since the function is now analytic there. (In Ref. [16] we did the expansion around $n = 1$, and we did, in fact, remove the F_H^{sub} term, Eq. (4). See Eq. (6.11) there.) The integral term in Eq. (20) is independent of T , so the leading contribution to the entropy comes from the third derivative term, allowing us to immediately obtain, as before,

$$\Delta F_H = -\frac{2}{15}(\pi a)^3 T^4, \quad aT \ll \sqrt{\lambda_0}, 1. \quad (21)$$

This is the well known strong-coupling low-temperature limit [15,16].

The above, of course, corresponds to a positive entropy. But this analysis presumed that aT was the smallest scale in the problem. However, we have another parameter, $\xi = \alpha \sqrt{\frac{3}{2\lambda_0}}$, which could be large if $\lambda_0 \ll \alpha^2$. The analysis given in Ref. [16] is unchanged, and results in the formula

$$\Delta F_H = \left(\frac{2\lambda_0}{3}\right)^2 \frac{1}{\pi a} \left[\frac{\xi^2}{12} - \ln \xi - \Re \psi \left(1 + \frac{i}{\xi}\right) \right], \quad \alpha \ll 1, \xi \sim 1. \quad (22)$$

Here ψ is the digamma function. (An alternative derivation is given in Appendix A of Ref. [17].) This function is plotted in Fig. 3 of Ref. [16] and Fig. 1 of Ref. [17]. See Fig. 1 here. Evidently, the entropy, the negative derivative of the free energy with respect to temperature, goes negative for sufficiently weak coupling (large ξ), as is seen from the analytic limiting behavior:

$$\xi \gg 1 : \quad \Delta F_H \sim \frac{2}{9} \lambda_0 \pi a T^2, \quad \sqrt{\lambda_0} \ll aT \ll 1. \quad (23)$$

The TE contribution to the entropy is always negative, so the total entropy turns negative for sufficiently small coupling.

4.2. Abel-Plana analysis

The derivation of the same result must be achievable directly from the Abel-Plana form (6), since the Euler-Maclaurin formula is derivable from the Abel-Plana expression. It is a bit subtle, because we have to worry about the appropriate branch of the phase, but actually very simple.

First, we use Eq. (17) with the replacement x by ix . (Again, the leading odd term comes from $l = 1$.) This gives the predominant term in the phase, ($x \ll 1, x^2/\lambda_0 \sim 1$)

$$\arg \left[\frac{2}{3} \lambda_0 - \left(1 + \frac{7}{15} \lambda_0\right) x^2 + i \frac{4}{9} \lambda_0 x^3 \right] = \arctan \left[\frac{\frac{2}{3} x^3}{1 - \frac{3x^2}{2\lambda_0}} \right]. \quad (24)$$

The TM free energy thus reads for low T

$$\Delta F_H = - \left(\frac{2\lambda_0}{3}\right)^2 \frac{1}{\pi a} \frac{3\xi^3}{\alpha^3} \int_0^{\infty} dz \frac{1}{e^{2\pi z/\xi} - 1} \arctan \left[\frac{\frac{2}{3} \left(\frac{\alpha}{\xi}\right)^3 z^3}{1 - z^2} \right] \quad (25a)$$

$$\rightarrow - \left(\frac{2\lambda_0}{3}\right)^2 \frac{2}{\pi a} P \int_0^{\infty} dz \frac{1}{e^{2\pi z/\xi} - 1} \frac{z^3}{1 - z^2}, \quad \alpha \ll 1. \quad (25b)$$

These expressions require some explanation. For the first line, we remind the reader that, because of our choice of the branch of the arctangent to be the usual one, there is a discontinuity in the integrand

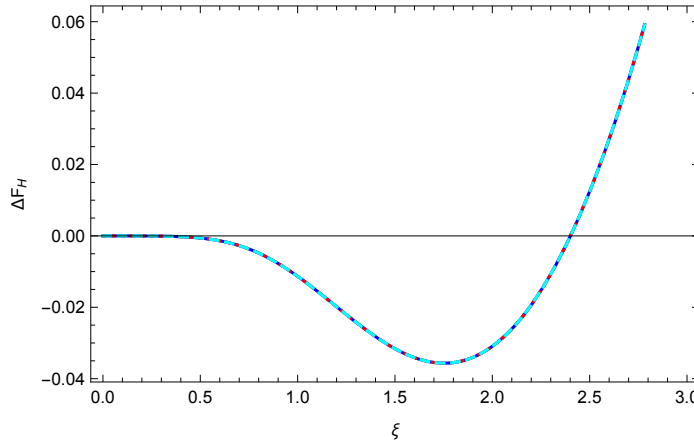


Figure 1. The TM free energy for low temperature in terms of $\xi = \alpha\sqrt{3/(2\lambda_0)}$. Shown are the coincident results for the formula (22), and for Eq. (25a) for $\alpha = 0.1$ and $\alpha = 0.01$. Plotted is the free energy apart from a factor of $(2\lambda_0/3)^2/(\pi a)$. Although the slope is negative (positive entropy) for small ξ (strong coupling), it is positive (negative entropy) for large enough ξ (weak enough coupling).

at $z = 1$, but of course this is integrable. We need, for stability, to evaluate the integral by taking a principal value there. In the second line, we have replaced $\arctan y$ by y , appropriate for small α , and the resulting singularity at $z = 1$ is integrated by taking a principal value. Then, numerically, both forms exactly agree with the previous formula (22), as Fig. 1 shows. The figure shows that for sufficiently weak coupling, the low-temperature entropy turns negative.

It is very easy (much easier than in Sec. 4.1) to extract the weak-coupling limit at low temperature, $\xi \rightarrow \infty$. The crucial observation is that (25b) receives contributions from only large $z \sim \xi$ when the latter is large, so the last factor in the integrand is merely $-z$ and then the integral gives the result (23) immediately. Note that the oddness of the arctangent around $z = 0$ is crucial here; were there a discontinuity in the argument function at $z = 0$, the $T \rightarrow 0$ limit would not exist.

5. High temperature

We showed in Refs. [16,17] that the leading behaviors for high temperature of the TM free energy and entropy are

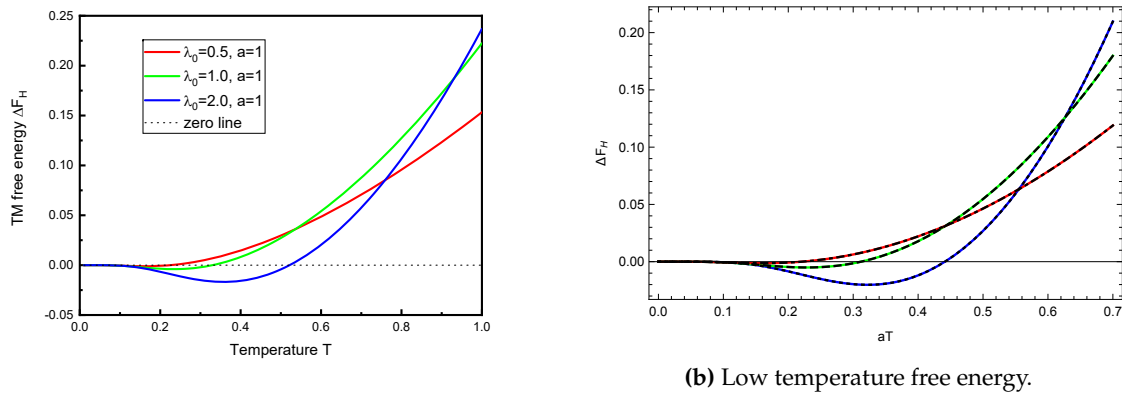
$$F_H \sim \frac{\lambda_0}{18} \pi a T^2, \quad S_H = -\frac{\partial}{\partial T} F_H \sim -\frac{\lambda_0}{18} \alpha, \quad \alpha = 2\pi a T \gg 1, \lambda_0. \quad (26)$$

Again, it is remarkable that this is first-order in the coupling. This same behavior was found in Ref. [18]. (If $\lambda_0 \gg 2\pi a T \gg 1$, the entropy becomes positive [15].) Here, we have made the universal subtraction of the term F_H^{sub} , but that should not alter the conclusion, because that contribution to the entropy is subdominant at high temperature. (Indeed, we dropped coupling-independent terms in Ref. [17].)

In Ref. [17] we worked out the leading high-temperature form for the free energy starting from the Euclidean frequency expression (1) using the uniform asymptotic expansions for the Riccati-Bessel functions and the Chowla-Selberg formula. Here, it seems to be much harder to use the uniform asymptotics on the highly oscillatory real-frequency Bessel functions appearing in the Abel-Plana expressions.

6. Numerical analysis

In principle, it seems that the Abel-Plana formula (6), which is finite, should be directly evaluated to obtain the free energy for any temperature and coupling strength. (It is not possible to do so starting from the Euclidean form (16), because this still contains divergences.) The difficulty is that the phase



(a) Exact free energy.

(b) Low temperature free energy.

Figure 2. The TM free energy (in units of $1/a$) computed from the exact formula (6) (left panel), or the low-temperature formula (22) or (25b) (right panel) plotted as a function of aT for the same intermediate values of λ_0 , $\lambda_0 = 0.5, 1$, and 2 , in increasing order on the right side of each figure. Although the low-temperature formula would not seem to be applicable here, since the temperature is not particularly low, it gives results which are qualitatively identical to the exact free energy seen in Fig. 2a, with significant deviations apparent only at higher T .

(8) becomes an extremely oscillatory function for $x > \nu$. Nevertheless, the sum and integral can be carried out for intermediate values of λ_0 and T with moderate computing resources.

In the numerical calculations, the behaviors of the phase in the vicinity of the singularities have to be carefully considered. When the coupling λ_0 is small, contributions to the free energy near these singularities are significant. Here, we have carried out the evaluations with sufficient precision to achieve reliable results, limited only by available hardware.

Fig. 2a shows the TM free energy for different moderate values of λ_0 , as a function of temperature. What is truly remarkable is how similar these curves are to those given by the low-temperature formula (22) which, despite its apparent inapplicability, is shown in Fig. 2b. Apparently, then, the numerical results shown in Fig. 2a still largely inhabit the low-temperature regime. This is not, perhaps, so surprising, since the validity of the replacement in Eq. (25b) demands $aT \ll 1$, not $a \ll 1$.

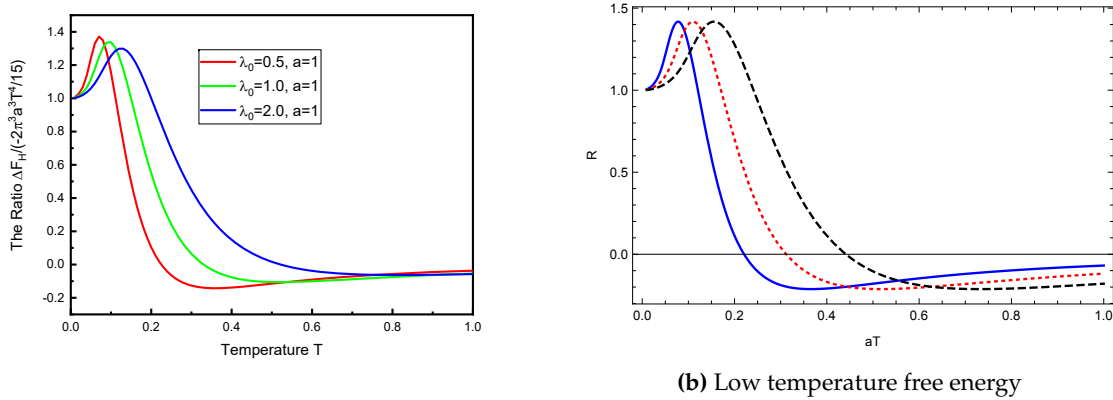
In Fig. 3a we compare the computed TM free energy to the strong-coupling low-temperature result (21). This is qualitatively very similar to that obtained by taking the ratio of Eqs. (22) and (21), as seen in Fig. 3b. Again, this demonstrates that the low temperature description extends to quite large temperatures. To put this into perspective, it might help to note that $aT = 1$ corresponds, at room temperature, to a sphere radius of $a = 8 \mu\text{m}$.

The weak-coupling regime for low temperature is explored in Fig. 4a. The comparison here is with Eq. (23). Of course, this agrees with that obtained from (22), as demonstrated in Fig. 4b. The low-temperature regime for moderate couplings is explored in Fig. 5a. Again, this agrees with the low-temperature free energy (22), as shown in Fig. 5b.

Finally, we compare in Fig. 6 the exact free energy relative to Eq. (15). We see that the weak-coupling formula is recovered as the coupling goes to zero, and that the ratio tends to one as the temperature increases, consistent with Eq. (26).

7. Conclusions

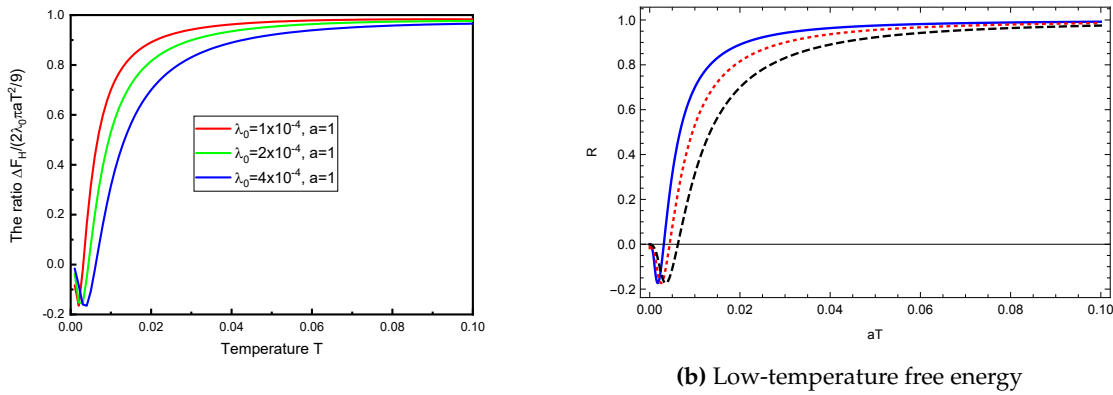
In this paper, we have re-examined the question of negative entropy for a spherical plasma-shell. We confirm the results first found in Ref. [16], using now a uniform subtraction of an irrelevant (infrared) divergent term, basing our re-analysis largely on the Abel-Plana representation of the free energy. Most interesting is that the leading anomalous terms (those corresponding negative entropy) are captured by the weak-coupling limit, which we also rederive here. In Fig. 7 we show the weak



(a) Exact free energy

(b) Low temperature free energy

Figure 3. TM free energy relative to the strong-coupling low-temperature limit. The left panel shows the exact TM free energy as a function of temperature T (in units of $1/a$) relative to the strong-coupling low-temperature limit (21), for various values of the coupling λ_0 . For very low temperature, the free energy agrees with the limit (21). The nonmonotonicity is quite striking. The right panel shows the ratio R of Eq. (22) to (21) as a function of aT . It is seen that the general low-temperature expression (22) captures most of the behavior shown in Fig. 3a. The different curves in Fig. 3b correspond to the same values of the coupling as in Fig. 3a, namely: $\lambda_0 = 0.5$ (blue, solid), $\lambda_0 = 1$ (red, dotted), $\lambda_0 = 2$ (black, dashed).



(a) Exact free energy

(b) Low-temperature free energy

Figure 4. The behavior of the TM free energy for low temperatures (in units of $1/a$), for even smaller values of the coupling, relative to the limiting value for low temperature and very small λ_0 , Eq. (23). The left panel shows the exact free energy, while the same ratio R is plotted in the right panel, except that the TM free energy is computed from the general low temperature expression (22). The different curves are for the same values of λ_0 as in Fig. 4a: $\lambda_0 = 10^{-4}$ (blue, solid), $\lambda_0 = 2 \times 10^{-4}$ (red, dotted), $\lambda_0 = 4 \times 10^{-4}$ (black, dashed). The fact that F_H turns negative for very small temperatures reflects the limit (21).

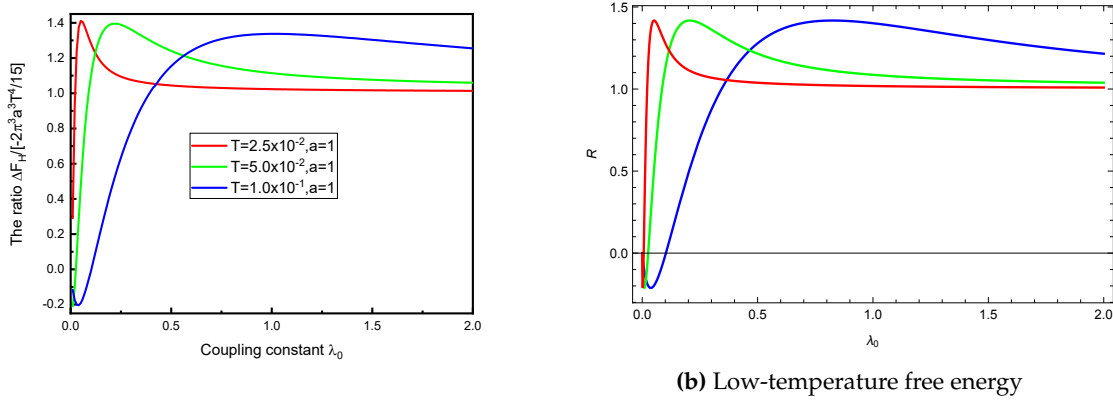


Figure 5. The left panel shows the ratio of the exact TM free energy to the strong-coupling, low-temperature limit (21) for relatively low temperatures, as a function of λ_0 . The reversal of sign for low λ_0 reflects the transition from the regime where Eq. (23) applies to the strong-coupling, low-temperature limit (21). The right panel shows the same ratio, except instead of the exact free energy, the general low-temperature expression (22) is used, for the same values of temperature. The two graphs are nearly indistinguishable. In both panels, the different curves correspond to the temperatures $aT = 2.5 \times 10^{-2}, 5 \times 10^{-2}, 1 \times 10^{-1}$, from bottom to top on the right of each panel.

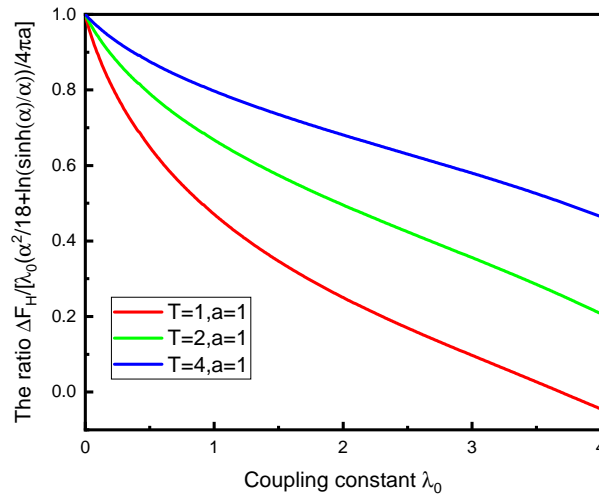


Figure 6. The free energy (6) compared to the $O(\lambda_0)$ approximation (15). For small coupling, the ratio approaches unity, and the curves become flatter for increasing temperature, consistent with the limiting form (26).

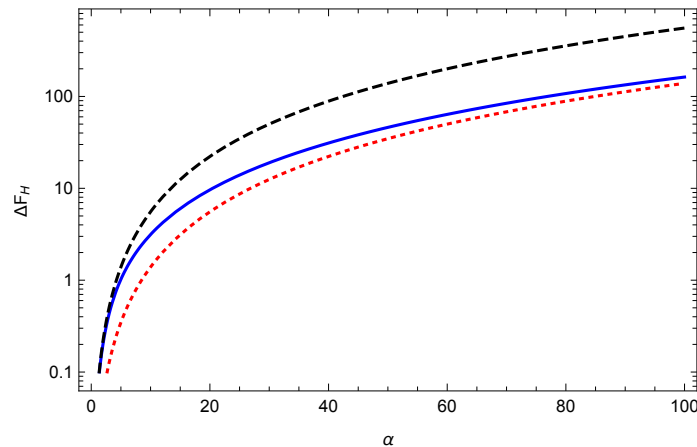


Figure 7. The $O(\lambda_0)$ contribution to the free energy (blue, solid), given by Eq. (15), with the prefactor $\lambda_0/(\pi a)$ pulled out, compared to the limiting forms (23) (low temperature, black, dashed) and (26) (high temperature, red, dotted).

coupling TM free energy (15) compared to the low and high temperature limits, given in Eqs. (23) and (26), respectively. The weak-coupling contribution to the entropy is always negative.

Since the anomalous behavior seems concentrated in the $O(\lambda_0)$ term, one might be tempted to argue it should be subtracted from the free energy [21]. After all, at zero temperature, such terms are frequently recognized as “tadpole” terms and are often omitted as unphysical. And for a dielectric ball, at zero temperature, the “bulk subtraction” also removes automatically the linear term in $(\epsilon - 1)$ [22]. Here, however, such a subtraction would ruin the limit to strong coupling, which has been understood for many years [15]; see, for example, Eq. (21). The analytic structure of the theory in the coupling constant is rather rigid, so *ad hoc* subtractions are not allowed. This point was made at the end of Ref. [16].

In any event, the anomalous behavior is not confined to weak coupling, as the numerical analysis summarized in Sec. 6 shows. Therefore, the occurrence of negative entropy here is hard to deny. These remarkable findings may have profound implications for our understanding of statistical mechanics and quantum field theory.

Author Contributions: Y.L, K.A.M., and P.P. contributed equally to this paper. L.L. contributed to the numerical analysis.

Funding: This research was funded by the U.S. National Science Foundation, grant numbers 1707511, 2008417.

Acknowledgments: We thank Gerard Kennedy, Steve Fulling, and Michael Guo for collaborative assistance.

Conflicts of Interest: The authors declare no conflicts of interest.

Abbreviations

The following abbreviations are used in this manuscript:

TE Transverse electric
TM Transverse magnetic

References

1. Schrödinger, E. *What is Life—the Physical Aspect of the Living Cell*. Cambridge University Press, 1944.
2. Cvetic, M., Nojiri, S., and Odintsov, S.D. Black hole thermodynamics and negative entropy in de Sitter and anti-de Sitter Einstein-Gauss-Bonnet gravity. *Nucl. Phys. B* **2002**, *628*, 295–330.
3. Nojiri, S. and Odintsov, S.D. The Final state and thermodynamics of dark energy universe. *Phys. Rev. D* **2004**, *70*, 103522.
4. Brevik, I., Ellingsen, S.A., and Milton, K.A. Thermal corrections to the Casimir effect. *New J. Phys.* **2006**, *8*, 236.

5. Bezerra, V.B., Klimchitskaya, G.L., Mostepanenko, V. M., and Romero, C. Lifshitz theory of atom-wall interaction with applications to quantum reflection. *Phys. Rev. A* **2008**, *78*, 042901.
6. Canaguier-Durand, A., Maia Neto, P. A., Lambrecht, A., and Reynaud, S. Thermal Casimir effect in the plane-sphere geometry. *Phys. Rev. Lett.* **2010**, *104*, 040403.
7. Canaguier-Durand, A., Maia Neto, P.A., Lambrecht, A., and Reynaud, S. Thermal Casimir effect for Drude metals in the plane-sphere geometry. *Phys. Rev. A* **2010**, *82*, 012511.
8. Bordag, M. and Pirozhenko, I.G., Casimir entropy for a ball in front of a plane. *Phys. Rev. D* **2010**, *82*, 125016.
9. Rodriguez-Lopez, P. Casimir energy and entropy in the sphere–sphere geometry. *Phys. Rev. B* **2011**, *84*, 075431.
10. Rodriguez-Lopez, P. Casimir energy and entropy between perfect metal spheres. In *Quantum Field Theory Under the Influence of External Conditions (QFEXT11)*, *Int. J. Mod. Phys.: Conf. Ser.* **2012**, *14*, 475-484.
11. Milton, K.A., Guérout, R., Ingold, G.-L., Lambrecht, A., and Reynaud, S. Negative Casimir entropies in nanoparticle interactions. *J. Phys.: Condens. Matter* **2015**, *27*, 214003.
12. Ingold, G.-L., Umrath, S., Hartmann, M., Guérout, R., Lambrecht, A., Reynaud, S., and Milton, K.A. Geometric origin of negative Casimir entropies: A scattering-channel analysis. *Phys. Rev. E* **2015**, *91*, 033203.
13. Li, Y., Milton, K.A., Kalauni, P., and Parashar, P. Casimir self-entropy of an electromagnetic thin sheet. *Phys. Rev. D* **2016**, *94*, 085010.
14. Milton, K.A., Li, Y., Kalauni, P., Parashar, P., Guérout, R., Ingold, G.-L., Lambrecht, A., and Reynaud, S. Negative entropies in Casimir and Casimir-Polder interactions. *Fortschr. Phys.* **2017**, *65*, 1600047.
15. Balian, R. and Duplantier, B. Electromagnetic waves near perfect conductors. 2. Casimir effect. *Ann. Phys. (N.Y.)* **1978**, *112*, 165–208.
16. Milton, K.A., Kalauni, P., Parashar, P., and Li, Y. Casimir self-entropy of a spherical electromagnetic δ -function shell. *Phys. Rev. D* **2017**, *96*, 085007.
17. Milton, K.A., Kalauni, P., Parashar, P., and Li, Y. Remarks on the Casimir self-entropy of a spherical electromagnetic δ -function shell. *Phys. Rev. D* **2019**, *99*, 045013.
18. Bordag, M. and Kirsten, K. On the entropy of a spherical plasma shell. *J. Phys. A* **2018**, *51*, 455001.
19. Bordag, M. Free energy and entropy for thin sheets. *Phys. Rev. D* **2018**, *98*, 085010.
20. Parashar, P., Milton, K.A., Shajesh, K.V., and Brevik, I. Electromagnetic δ -function sphere. *Phys. Rev. D* **2017**, *96*, 085010.
21. Graham, N., Jaffe, R.L., Khemani, V., Quandt, M., Schröder, O., and Weigel, H. The Dirichlet Casimir problem. *Nucl. Phys. B* **2004**, *677*, 379-404.
22. Milton, K.A., Parashar, P., Brevik, I., and Kennedy, G. Self-stress on a dielectric ball and Casimir–Polder forces. *Ann. Phys. (N.Y.)* **2020**, *412*, 168008.